INTERNATIONAL JOURNAL OF HYDROGEN ENERGY 35 (2010) 11387–11396

Available at www.sciencedirect.com

ScienceDirect

journal homepage: www.elsevier.com/locate/he

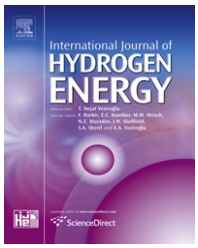

Inhibition effect of newly synthesized heterocyclic organic molecules on corrosion of steel in alkaline medium containing chloride

*M.A. Ameer, A.M. Fekry**

Chemistry Department, Faculty of Science, Cairo University, Giza 12613, Egypt

ARTICLE INFO

Article history:
Received 21 May 2010
Received in revised form
12 July 2010
Accepted 13 July 2010
Available online 13 August 2010

Keywords:
Corrosion inhibition
EIS
Polarization
SEM
Steel

ABSTRACT

Two new organic compounds were tested experimentally as inhibitors for mild steel in NaOH in presence of NaCl by electrochemical and hydrogen evolution techniques. Results demonstrated that the two inhibitors show an adsorption on steel surface according to Langmuir adsorption isotherm. The inhibition efficiency increases with increasing inhibitor concentrations to attain a maximum value at 1.0 mM for compound I and at 6.0 mM for compound II, respectively. The results were confirmed by surface examination via scanning electron microscope.

Published by Elsevier Ltd on behalf of Professor T. Nejat Veziroglu.

1. Introduction

In some fuel cells mild steel can be used as shims and cell case. Fuel tanks located outside body and/or frame must be enclosed in a steel tube frame constructed of mild steel tubing. The corrosion of steel has received a considerable amount of attention as a result of its industrial relevance. Steel remains in the passive state in alkaline solution but various contaminants have a detrimental effect on passivity. Among them, chloride ions are the most common ones and localized corrosion triggers when chlorides reach the metal surface [1]. The use of corrosion inhibitors is probably more attractive from the point of view of economics and ease of application [2]. Reviews of the most commonly used corrosion inhibitor types and the various possible mechanisms of inhibition have been recently published [3–5]. Considering the inhibition of corrosion of mild steel alloy, the processes of the metal corrosion (active dissolution) and of the hydrogen embrittlement have to be taken into account. The effective inhibitors should suppress both the corrosion and the hydrogen charging, not intensifying any of them. The detrimental effect of chloride ions to the passive layer naturally formed on iron exposed to alkaline environments has been extensively reported in the literature. Many authors have investigated the chloride threshold values for the corrosion of steel in concrete, mortars and alkaline solutions [6–8]. In alkaline solutions the threshold value relative to the OH^- content, given as $[Cl^-]/[OH^-]$ ratio presents a mean value around 0.6 [7]. Most of the efficient inhibitors used in industry are organic compounds having multiple bonds in their molecules which mainly contain nitrogen and sulphur atoms through which they are

* *Corresponding author*. Tel.: +20 2 0101545331; fax: +20 2 37832666.
E-mail address: hham4@hotmail.com (A.M. Fekry).
0360-3199/$ – see front matter Published by Elsevier Ltd on behalf of Professor T. Nejat Veziroglu.
doi:10.1016/j.ijhydene.2010.07.071

adsorbed on the metal surface. Compounds with functional groups containing oxygen, nitrogen and sulphur have the ability to form complexes with iron. They have been reported to act as effective inhibitors to the surface of steel by means of their competitive adsorption through the surface complex formation. In practice corrosion can never be stopped but hindered to a reasonable level. Organic compounds used as inhibitors act through a process of surface adsorption, so the efficiency of an inhibitor depends on [2,3]: the chemical structure of the organic compound, the surface charge of the metal, and the type of interactions between the organic molecule and metal surface. Existing data reveal most inhibitors to act by adsorption on the metal surface through heteroatom such as nitrogen, oxygen and sulphur, double bonds, triple bonds or aromatic rings which tend to form stronger coordination bonds. Compounds with π-bonds generally exhibit good inhibitive properties, the electrons for the surface interaction being provided by the π-orbitals [3]. The main aim of this research work is to study the electrochemical behavior and hydrogen evolution of mild steel in different concentrations of organic inhibitors (newly synthesized heterocyclic compounds) in 1.0 M NaOH + 0.1 M NaCl solutions as shown in Scheme 1. These compounds are required for several chemical transformations as well as our medicinal chemistry programs. The two compounds exhibit anti-Alzheimer and anti-cyclooxygenase enzyme type 2 (COX2) activities [8]. Also, the effect of temperature is studied for compound I. Different techniques were employed such as potentiodynamic polarization and electrochemical impedance spectroscopy (EIS).

2. Experimental

Mild steel rod (C = 0.31%; Si = 0.21%; Mn = 0.81%; P = 0.014%; S = 0.017%; Cu = 0.06%; Cr = 0.02%; Mo = 0.01%; Ni = 0.02%; V = 0.002% by weight) was tested in the present study with its cross-sectional area of 0.46 cm^2. The surface of the test electrode was mechanically abraded by emery papers with 400 up to 1000 grit to ensure the same surface roughness, degreased in acetone, rinsed with ethanol and dried in air. The test solution (blank) is 1.0 M NaOH + 0.1 M NaCl containing different concentrations of 4-(4-methoxyphenyl)-6-thioxo-1,6-dihydro-2,3′-bipyridine-5-carbonitrile (compound I) or 4-(4- methoxyphenyl)-6-(thiophen-2-yl)-2-thioxo-1,2-dihydropyridine-3-carbonitrile(compound II). The concentration range is 0.01–10 mM. The chemical structure of the two investigated organic inhibitors is given below [8]:

The cell used was a typical three-electrode one fitted with a large platinum sheet of size 15 × 20 × 2 mm as a counter electrode (CE), saturated calomel (SCE) as a reference electrode (RE) and the alloy as the working electrode (WE). The impedance diagrams were recorded at the free immersion potential (OCP) by applying a 10 mV sinusoidal potential

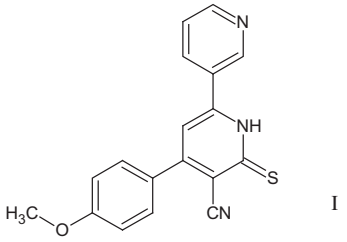

I

Formula Weight = 319.38032

4-(4-methoxyphenyl)-6-thioxo-1,6-dihydro-2,3'-bipyridine-5-carbonitrile

Molecular Formula = $C_{18}H_{13}N_3OS$

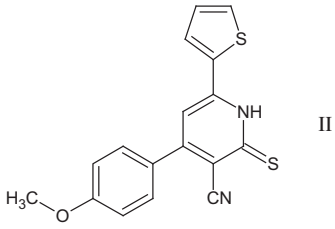

II

Formula Weight = 324.41998

4-(4-methoxyphenyl)-6-(thiophen-2-yl)-2-thioxo-1,2-dihydropyridine-3-carbonitrile

Molecular Formula = $C_{17}H_{12}N_2OS_2$

Scheme 1. The structure of compound I & II.

through a frequency domain from 30 kHz down to 100 mHz. Polarization and EIS measurements were carried out using the electrochemical workstation IM6e Zahner-electrik GmbH, Germany. The scan rate was 30 mV min^{-1}. Hydrogen evolution experiments were undertaken using gasometric assembly similar to that described in the literature [9–11]. The assembly is essentially an apparatus that measures the volume of gas evolved from a reaction system. It consists of essentially two-necked round bottom flask which serves as the reaction medium containing the corrodent and the metal coupons. Others are a separating funnel, a burette fitted with taps and an outer glass jacket that serves as a water condenser. In this technique, 100 ml of different test solutions were introduced into a reaction vessel which was connected to a burette through a delivery tube. To study the effect of temperature, the cell was immersed in water thermostat in blank without/with 0.01 mM compound I and II in the temperature range of 288 K–328 K. The SEM micrographs were collected using a JEOL JXA-840A electron probe microanalyzer.

3. Results and discussion

3.1. *Effect of inhibitor concentration*

The influence of Cl^- ions on the passivity breakdown of mild steel can be interpreted as a balance between two processes competing on the metal surface: stabilization of the passive film by OH^- adsorption and disruption of the film by Cl^- ions adsorption. When the activity of chlorides overcomes that of hydroxyls, corrosion occurs [12]. During corrosion, the reversible formation of $Fe(OH)_{ad}$ adsorbed on the bare metal is the first stage of the repassivation process followed by the oxidation of this layer to produce a thicker oxide film (passivating film) [13,14] according to the following sequence:

$$Fe + OH^- = FeOH^-_{ad} \quad (1)$$

$$FeOH^-_{ad} = FeOH_{ad} + e^- \quad (2)$$

$$FeOH_{ad} + OH^- = Fe(OH)_{2s} + e^- \quad (3)$$

$$Fe(OH)_{2s} + OH^- \rightarrow FeOOH_s + H_2O + e^- \quad (4)$$

In the presence of chloride ions, the $Fe(OH)_{ad}$ coverage decreases resulting in an increasing of the anodic dissolution of the metal when the following reactions occur

$$Fe + Cl^- = FeCl_{ad} + e^- \quad (5)$$

$$FeCl_{ad} = FeCl^+_{aq} + e^- \quad (6)$$

Fig. 1a,b represents the potentiodynamic polarization curves of steel in blank solution (1.0 M OH^-/0.1 M Cl^-) without and with different concentrations of inhibitor I and II, respectively, at 298 K. The data show that, the addition of inhibitor I or II does not affect well on the corrosion potential (E_{corr}) value. According to the electrochemical parameters (i_{corr}, E_{corr}, β_a and β_c) given in Table 1, it is obvious that the anodic Tafel slope (β_a) and cathodic Tafel slope (β_c) remain almost constant upon the addition of each inhibitor. These results indicate that, these inhibitors decrease the surface area for corrosion without affecting the mechanism of corrosion by merely blocking the reaction sites of the metal surface without changing the anodic and cathodic reaction mechanisms and only cause inactive of a part of surface with respect to the corrosion medium. The results indicate also, that the two compounds are mixed type inhibitors. For i_{corr} value, it was found to decrease so slightly till 1 mM then increases till 10 mM for compound I and decreases till 6 mM for compound II then increases slightly at 10 mM concentration. This means that compound I has the lowest corrosion rate at 1 mM and compound II at 6.0 mM concentration, however, compound I always has lower corrosion rate than compound II. The inhibition efficiency at different concentrations of the two

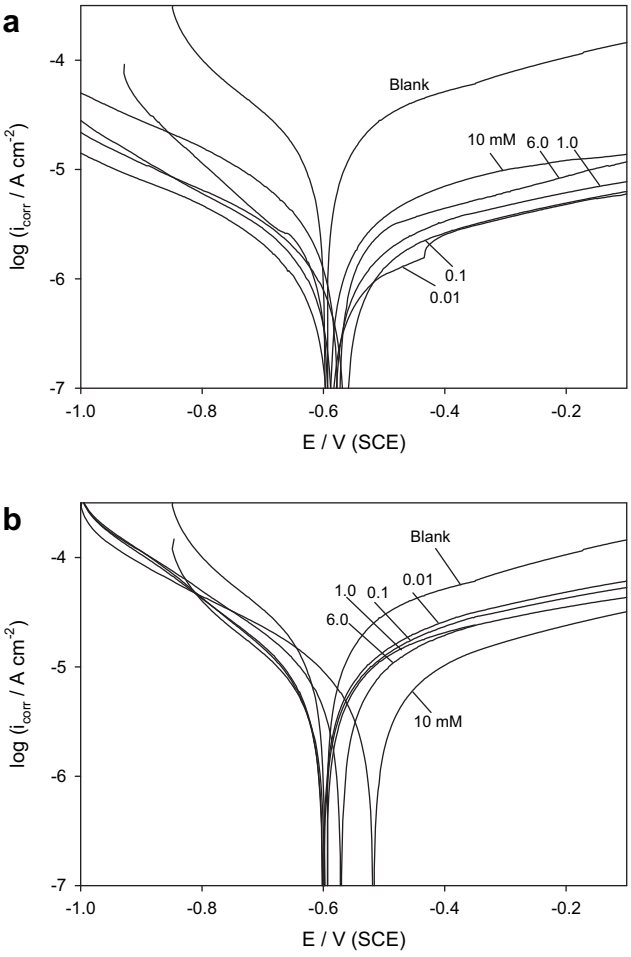

Fig. 1 – Potentiodynamic polarization curves of steel in blank solution without and with different concentrations of compound a) I and b) II at 298 K.

Table 1 – Corrosion parameters of mild steel alloy at different concentrations of compound I & II in blank solution, at 298 K.

Inhibitor	Conc.	i_{corr}	E_{corr}	β_a	β_c
	mM	μA cm^2	mV	mV/dec	mV/dec
I	0.0	2.060	−600	49.1	42.4
	0.01	0.228	−575	47.3	41.2
	0.1	0.227	−584	48.3	42.1
	1.0	0.226	−584	46.1	41.3
	6.0	0.240	−590	47.4	41.1
	10	0.270	−564	45.3	41.7
II	0.0	2.060	−600	49.1	42.4
	0.01	0.700	−600	41.5	38.3
	0.1	0.696	−597	40.8	38.1
	1.0	0.690	−597	40.1	37.9
	6.0	0.660	−571	41.6	37.9
	10	0.670	−518	42.9	37.4

inhibitors is calculated and tabulated in Table 2 using the following equation [3,15,16]:

$$IE\% = \frac{i^{\circ}_{corr} - i_{corr}}{i^{\circ}_{corr}} \times 100 \quad (7)$$

where i°_{corr} and i_{corr} are the corrosion current densities for steel electrode in absence and presence of inhibitors, respectively. As observed from Table 2, that inhibition efficiency (*IE*%) increases slightly till 1.0 mM and after that it decreases for compound I, however, it increases till 6.0 mM then decreases at 10 mM for compound II. Comparing the *IE*% values of the two inhibitors, we find that the order of inhibition is as follows: I > II.

The EIS experiments for steel traced at the rest potential in 1.0 M NaOH solution with Cl^- at different concentrations of compound I or II were shown in Fig. 2a,b and the observed fitted data are tabulated in Table 3. Fig. 2a,b shows that in all cases the impedance Bode plots display two maximum phase lags, indicating the presence of two time constants. According to this, our experimental impedance data were best fitted to an electrical equivalent circuit (EEC) shown in Fig. 3. EEC consists of two circuits from $R_1Z_WC_1$ and R_2C_2 parallel

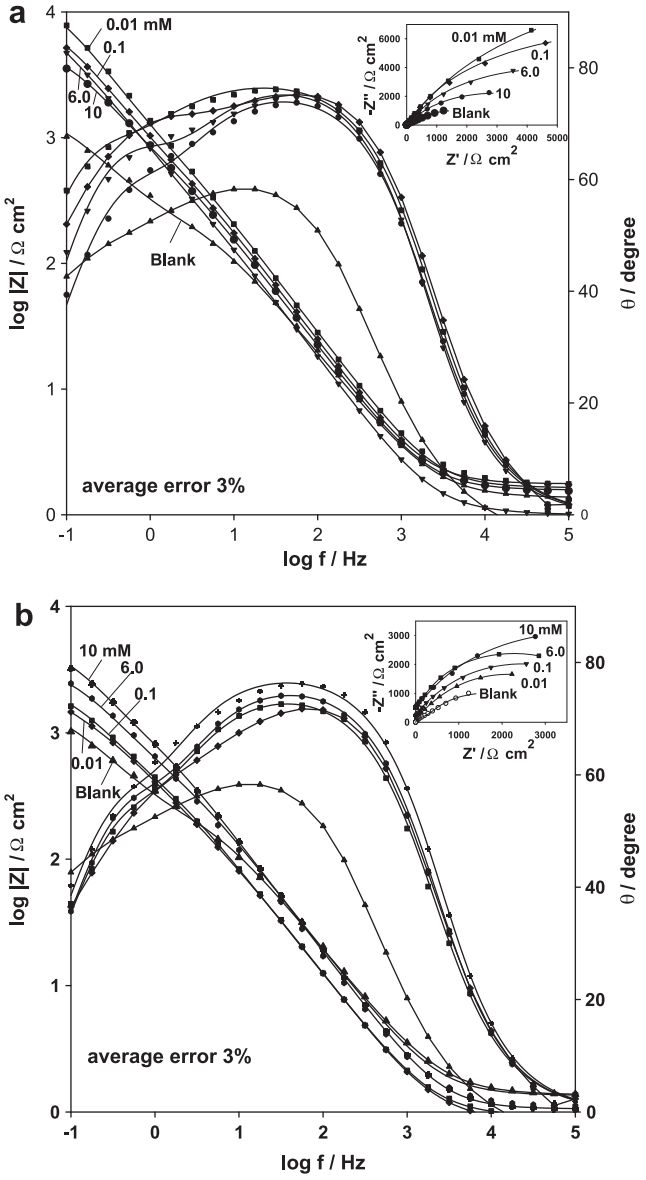

Fig. 2 – Bode and Nyquist plots for steel in blank without and with compound a) I and b) II in the blank, at 298 K.

Table 2 – Inhibition efficiencies of mild steel alloy at different concentrations of compound I & II in blank solution, at 298 K.

Inhibitor	$C_{inhibitor}$/mM	*IE*% H_2 evolution	*IE*% *EIS*	*IE*% Tafel
I	0.00	–	–	–
	0.01	85.87	93.88	88.93
	0.1	84.60	93.31	88.98
	1.0	84.98	93.69	89.03
	6.0	84.78	93.41	88.34
	10	83.60	93.19	86.89
II	0.00	–	–	–
	0.01	60.37	56.49	66.01
	0.1	60.00	57.08	66.21
	1.0	58.98	67.05	66.51
	6.0	54.78	67.04	67.96
	10	50.60	67.25	67.48

combination and the two are in series with the solution resistance (R_S). By this way C_1 is related to combinations from the capacitance of the outer layer and C_2 of the inner layer while R_1 is the resistance of the outer layer and R_2 of the inner layer [17]. Warburg impedance (Z_w) can be linked to ion diffusion through the passive film. This Warburg impedance indicates that the corrosion mechanism is controlled not only by a charge-transfer process but also by a diffusion process [18]. Z_w found to decrease with increasing concentration of compound I and increases with increasing concentration of compound II in the blank. Fitting procedures have shown that better agreement between the theoretical and experimental data (3% error) is obtained if a frequency-dependent constant phase element (CPE) is introduced instead of pure capacitor. Generally, the usage of CPE is due to frequency dispersion as a result of distribution of relaxation times and inhomogenities,

Table 3 – Equivalent circuit parameters of mild steel alloy at different concentrations of compound I & II in blank solution, at 298 K.

Inhibitor	$C_{inhibitor}$/mM	$R_S/\Omega\ cm^2$	$R_1/K\Omega\ cm^2$	$C_1/\mu F\ cm^{-2}$	$W/\Omega\ cm^2\ s^{-1/2}$	α_1	$R_2/k\Omega\ cm^2$	$C_2/\mu F\ cm^{-2}$	α_2
I	0.00	1.4	0.07	199.3	220	0.66	1.33	84.8	0.84
	0.01	1.8	0.56	56.6	310	0.68	22.3	42.5	0.82
	0.1	1.7	0.50	58.2	389	0.73	20.4	41.8	0.84
	1.0	1.4	0.55	60.5	370	0.68	21.7	40.7	0.86
	6.0	1.4	0.52	60.1	365	0.69	20.7	40.8	0.86
	10	1.4	0.32	64.3	350	0.68	20.2	38.8	0.86
II	0.00	1.4	0.07	199.3	220	0.66	1.33	84.8	0.89
	0.01	1.8	0.24	93.2	240	0.61	2.98	48.7	0.85
	0.1	1.8	0.24	93.0	254	0.60	3.02	45.9	0.87
	1.0	1.6	0.26	92.4	269	0.67	3.99	43.2	0.86
	6.0	1.6	0.26	91.7	280	0.63	3.99	42.7	0.88
	10	1.6	0.25	90.9	299	0.61	4.02	48.1	0.87

as well as static disorders such as porosity [19]. The impedance (Z_{CPE}) described by the expression [20]:

$$Z_{CPE} = 1/C(j\omega)^{\alpha} \quad (8)$$

where $0 \leq \alpha \leq 1$

The total reciprocal capacitance (C_T^{-1}) of the passive film is directly proportional to its thickness [20].

$$C_T^{-1} = C_1^{-1} + C_2^{-1} \quad (9)$$

From the data of Table 3, it is clear that both C_T^{-1} and R_T ($R_1 + R_2$) are nearly constant for compound I, but increase slightly for compound II. In general the values of C_T^{-1} and R_T are in the order of: I > II. The inhibition efficiency at different concentrations of the two inhibitors were calculated and tabulated in Table 2 using the following equation:

$$IE\% = \frac{R^T - R_T^{\circ}}{R_T} \times 100 \quad (10)$$

where R_T° and R_T are the total resistances for steel in absence and presence of inhibitors, respectively.

The inhibition efficiency of compound I is higher than that of II as shown in Fig. 4 and this is attributed to the electron rich environment on compound I than compound II. Such action could be explained through the lone pair of non-bonding electrons on N atom of pyridine ring in compound I, these electrons are freely liberated into the system. However, the electrons on S atom in compound II are restricted to be liberated due to they are involved into the aromatization of thiophene ring. Also, this is due to the pyridine ring is six membered ring in compound I whereas thiophene ring is five membered ring in compound II.

The corrosion of mild steel in blank solutions in the absence and presence of different concentrations of compound I or II was also investigated using the hydrogen evolution measurements. The corrosion rates of mild steel in the absence and presence of the additives were assessed by monitoring the volume of hydrogen gas evolved. Inhibition efficiency (*IE*%) from the hydrogen evolution measurements was obtained using the following equation [21–23]:

$$IE(\%) = (1 - V^{\circ}/V) \times 100 \quad (11)$$

where V° and V are the volumes (ml) of hydrogen evolved without and with inhibitor, respectively. The results obtained are presented in Table 2. Inhibition efficiency decreased with increasing concentration of the inhibitors + blank solution. The values of inhibition efficiency obtained from the hydrogen evolution method are lower than that obtained from Tafel and impedance measurements (EIS). This can be attributed to the difference in time required to form an adsorbed layer of the inhibitor on the metal surface that can inhibit corrosion.

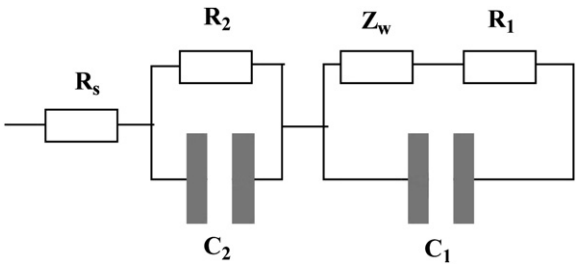

Fig. 3 – The electrical equivalent circuit model used in fitting the experimental EIS data.

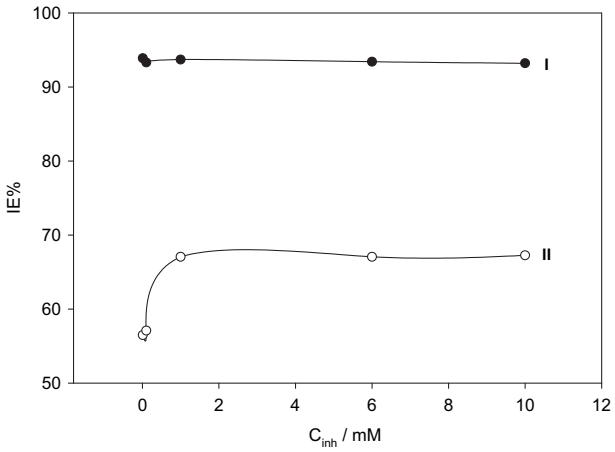

Fig. 4 – Variation of inhibition efficiency calculated from EIS measurements for steel in blank with different concentrations of compound I and II.

In alkaline solutions the reaction of hydrogen evolution can be written as:

$$H_2O + e^- = H_{ads} + OH^- \quad (12)$$

where H_{ads} represents a hydrogen atom adsorbed onto the cathode surface occurs predominantly by the Tafel reaction [24]:

$$H_{ads} + H_{ads} = H_2 \quad (13)$$

Alternatively, removal of H_{ads} might occur via Heyrovsky reaction [3]:

$$H_2O + H_{ads} + e^- = H_2O + OH^- \quad (14)$$

3.2. *Effect of immersion time*

EIS is a useful technique for long time tests, because they do not significantly disturb the system and it is possible to follow it over time [25]. The present work was carried out in blank containing 0.01 mM of compound I for 100 h. From EIS data, it is obvious that both R_T and C_T^{-1} values increased sharply during the initial 3 h and remained fairly constant afterward, Fig. 5. This means that the formation of inhibitor surface film, and inhibitor adsorption, on the electrode surface was fast and completed within 3 h. The results demonstrate that the *IE*% increases with increasing immersion time sharply during the initial 3 h and remained fairly constant afterward (Fig. 6). This is consistent with the synergistic effect of inhibitor (due to adsorption) and steel corrosion products to increase the protective power of the passive film and a compact adsorbed film of the inhibitor is formed on the steel surface [26]. Competitive adsorption is assumed to occur on the steel surface between the aggressive OH^- ions and the anions of the inhibitor molecule [27]. Fig. 7 reveals that the volume of H_2 evolved vary linearly with immersion time according to the relation ($V = kt$), where V is the volume of H_2 gas evolved at time 't' and 'k' is the rate constant of the H_2 evolution reaction. It is also observed from the figure that lesser H_2 gas was liberated from the mild steel surface on introduction of compounds I or II compared to the blank solution showing that both compound I and II actually inhibit the corrosion of mild steel in solution. The volume of H_2 evolved was found to decrease with increasing immersion time but increased with increase in the concentrations of compound I or II. The inhibition efficiency for mild steel corrosion in the absence and presence of inhibitors

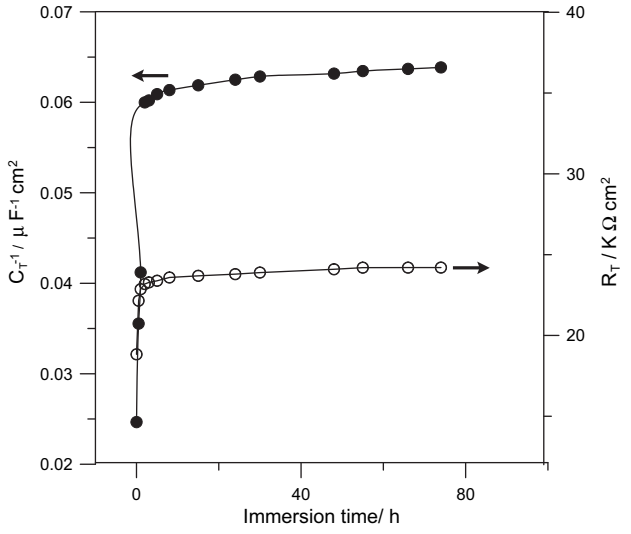

Fig. 5 – Dependence of C_T^{-1}, R_T on the immersion time for steel in blank with 0.01 mM of compound I at 298 K.

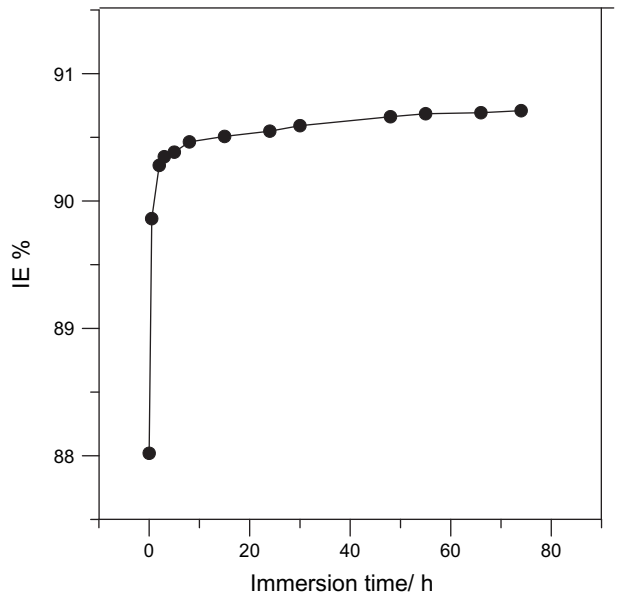

Fig. 6 – Dependence of *IE*% on the immersion time for steel in blank with 0.01 mM of compound I at 298 K.

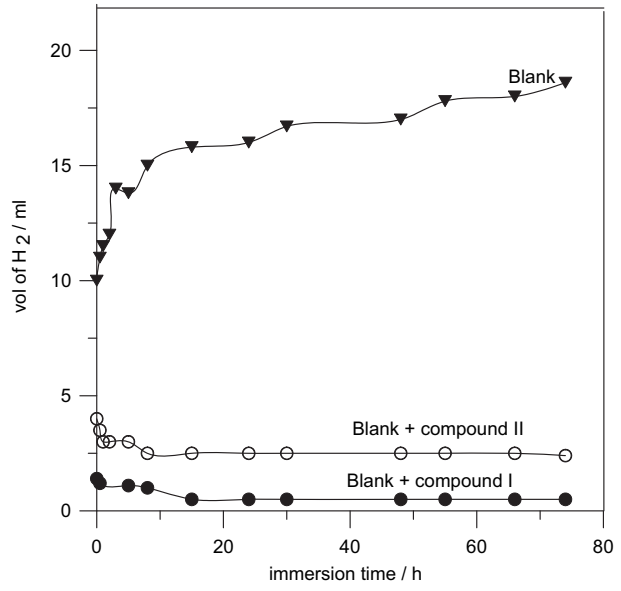

Fig. 7 – The variation of H_2 evolution gas with immersion time for steel in blank solution with and without compound I or II.

at different concentrations are presented in Table 2. The values of inhibition efficiency (*IE*%) follow nearly the same trend that observed from impedance and Tafel measurements. It decreases with increase in concentration of inhibitors but increased with increase in immersion time.

3.3. *Adsorption isotherm*

Data obtained from polarization measurements were tested graphically for fitting various isotherms including Langmuir, Frumkin and Temkin. The two compound gives the best fit with Langmuir isotherm (Fig. 8). According to this isotherm θ is related to inhibitor concentration.

$$\frac{C}{\theta} = \frac{1}{K_{ads}} + C \quad (15)$$

where θ is the surface coverage ((*IE*%)/100) of the inhibitor on the steel surface, *C* is inhibitor concentration and K_{ads} is the adsorption–desorption equilibrium constant. By plotting C/θ versus *C* at 298 K for the two inhibitors, straight lines were obtained as seen in Fig. 8. From the intercepts, K_{ads} values were calculated for the adsorption process. The equilibrium constant of adsorption is seen to be higher for compound I than II (2.36×10^4 M^{-1}) and (1.17×10^4 M^{-1}), respectively. However, the slopes of the relation show a little deviation from unity, this may result from the interactions between the adsorbed species on the metal surface [28]. The K_{ads} values may be taken as a measure of the strength of the adsorption forces between the inhibitor molecules and the metal surface [3]. Therefore, the strongest interaction between the double layer existing at the phase boundary, and the adsorbed molecules gives the highest *IE*% for compound I.

3.4. *Effect of temperature*

In order to gain more information about the type of adsorption and the effectiveness of the studied inhibitors at high temperatures, polarization and EIS experiments were performed at different temperatures (288–328 K) for the steel electrode in blank without and with 10^{-2} mM of compounds I and II. Fig. 9 (as an example) shows the Bode plots and Nyquist

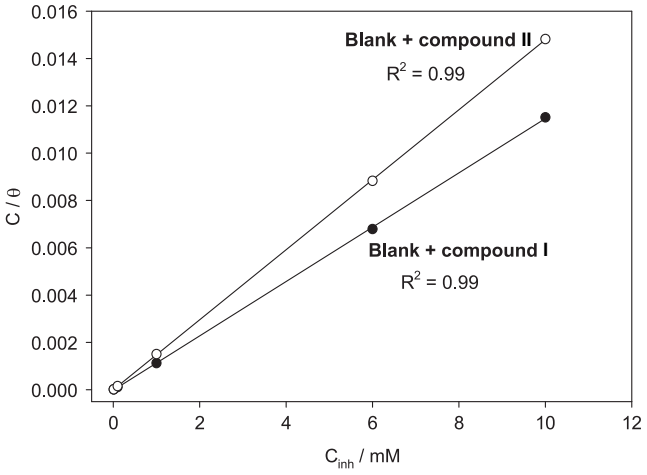

Fig. 8 – Langmuir adsorption isotherm of the two compounds on steel surface.

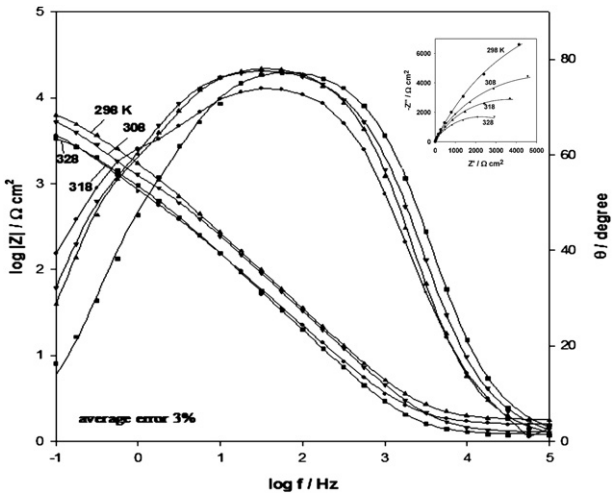

Fig. 9 – The impedance diagram of steel in blank with 0.01 mM of compound I at different temperatures represented as Bode and Nyquist plots.

plots for the steel electrode in blank with 0.01 mM of compound I at different temperatures. It has been observed from impedance plots that impedance values increase with decreasing temperature. Also, from Nyquist plots, it is found that the diameter of the semi-circles increases with decreasing temperature of the medium. It was observed that there is a diffusion phenomenon in the Nyquist plots. Thus, the appropriate model for fitting this data is as shown in Fig. 4.

A plot of log i_{corr}, obtained from polarization measurements, versus T^{-1} gives a straight line with a slope $-E_a/2.303R$, from which the activation energies were calculated (Fig. 10) using Arrhenius equation:

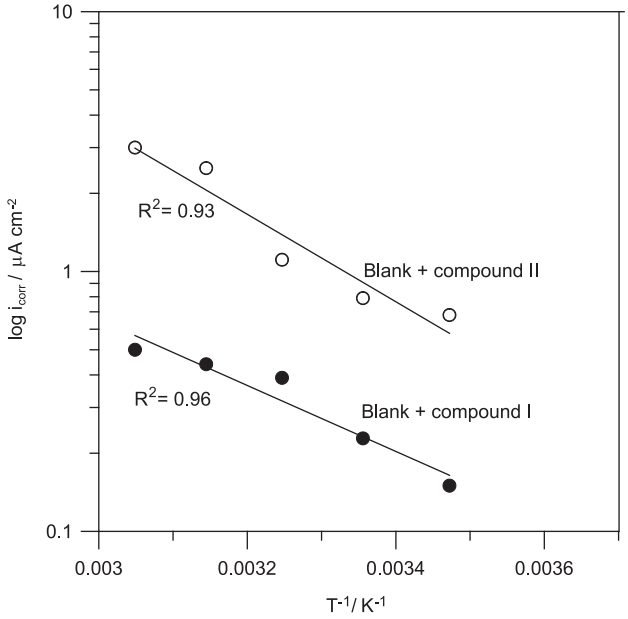

Fig. 10 – Arrhenius plot for steel in blank with 0.01 mM of compound I and II at different temperatures.

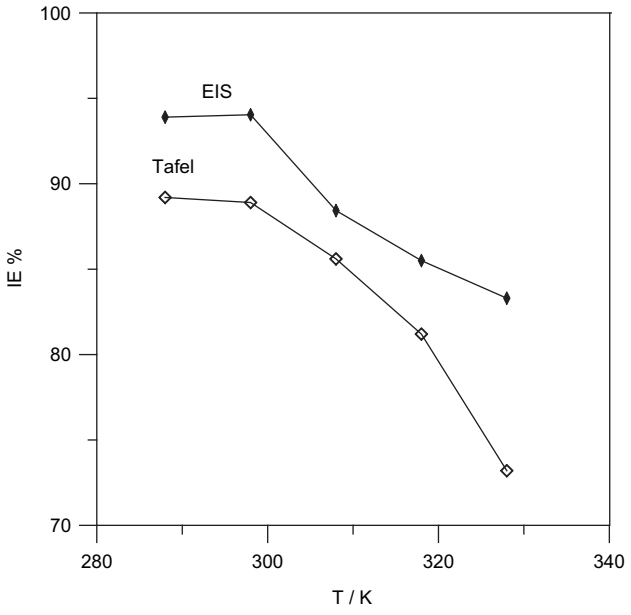

Fig. 11 – The variation of inhibition efficiencies calculated from Tafel and EIS for steel in blank containing 0.01 mM of inhibitor I at different temperatures.

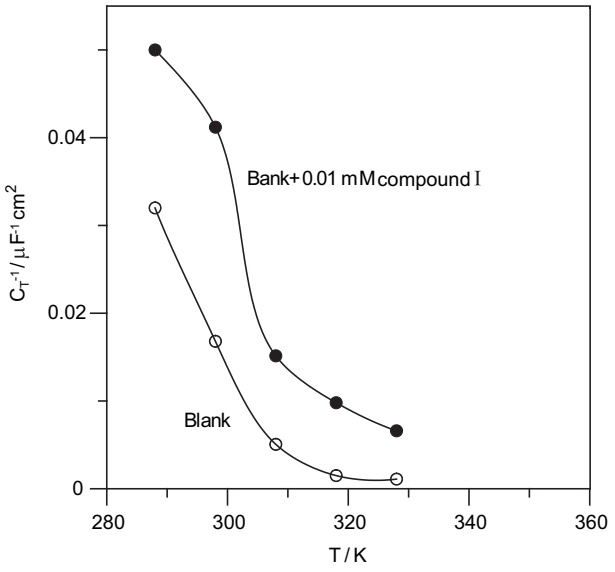

Fig. 13 – Dependence of C_T^{-1} on the temperature for steel in blank without and with 0.01 mM of compound I.

$$\log i_{corr} = A - E_a/2.303RT \quad (16)$$

where E_a is activation energy, R the universal gas constant and A the Arrhenius factor. The activation energies calculated for blank in presence of 0.01 mM of compounds I and II were 24.38 kJ mol^{-1} and 31.56 kJ mol^{-1}, respectively. The adsorption equilibrium constant K_{ads}, is related to the standard free energy, ΔG°_{ads}, with the following equation:

$$\log K_{ads} = \log\frac{1}{55.5} + \frac{\Delta G^{\circ}_{ads}}{2.303RT} \quad (17)$$

The relation between log K_{ads} and T^{-1} deduced ΔG°_{ads} which is −30.24 kJ mol^{-1} and −26.56 kJ mol^{-1} for steel in blank with 0.01 mM of compound I and II, respectively indicating that in blank solution the two compounds adsorb on steel surface via a physisorption-based mechanism [15]. This is also supported by the high molecular weight of the two compounds which shows better corrosion inhibition beside the fact that *IE*% of the investigated inhibitor decreases at higher temperatures (288–323 K). The negative value of ΔG°_{ads} indicating the spontaneous process and that the two compounds are strongly adsorbed into steel surface. So, the relatively high *IE*% may indicate a strong interaction of the two compounds with steel surface.

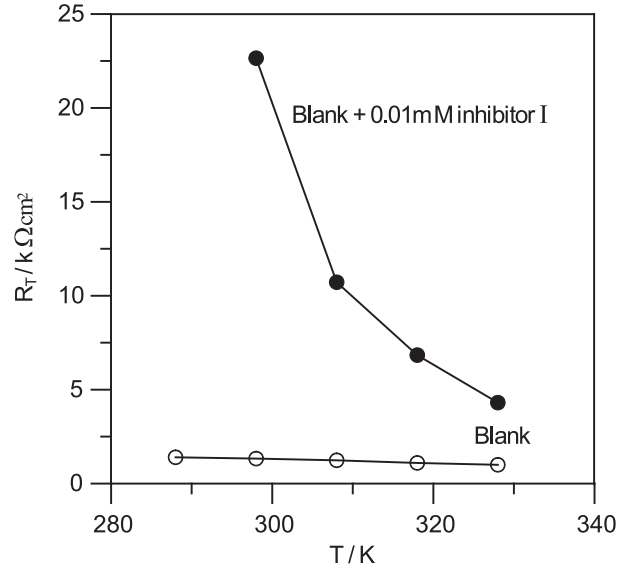

Fig. 12 – Dependence of R_T on the temperature for steel in blank without and with 0.01 mM of compound I.

By using the transition state equation [15]:

$$\log\left(\frac{i_{corr}}{T}\right) = \log\frac{R}{Nh} + \frac{\Delta S^{o}_{ads}}{2.303R} - \frac{\Delta H^{o}_{ads}}{2.303RT} \quad (18)$$

where N is the Avogadro's number and h is the Plank constant, a plot of log i_{corr}/T against T^{-1} yields a straight line and the standard enthalpy change ΔH^{o}_{ads} and standard entropy change ΔS^{o}_{ads} for the adsorption process can be evaluated. It was found that the magnitudes of both parameters are −35.6 kJ mol^{-1} and −82.5 J K^{-1} mol^{-1} for blank containing compound I, −18.5 kJ mol^{-1} and −99.5 J K^{-1} mol^{-1} for blank with compound II, respectively.

Fig. 11 shows the variation of inhibition efficiencies calculated from Tafel and EIS for steel in blank solution containing 0.01 mM of compound I at different temperatures. It is clear from the figure that at low temperatures (<300 K) the efficiency is almost constant and decreases rapidly with increasing temperatures which confirm the previous results. Such behavior can be interpreted on the basis that an increase in temperature resulted in desorption of some adsorbed active centers of compounds I and II molecules from the metal surfaces. This type of inhibitor retards corrosion at ordinary temperatures but inhibition is diminished at higher temperatures [2].

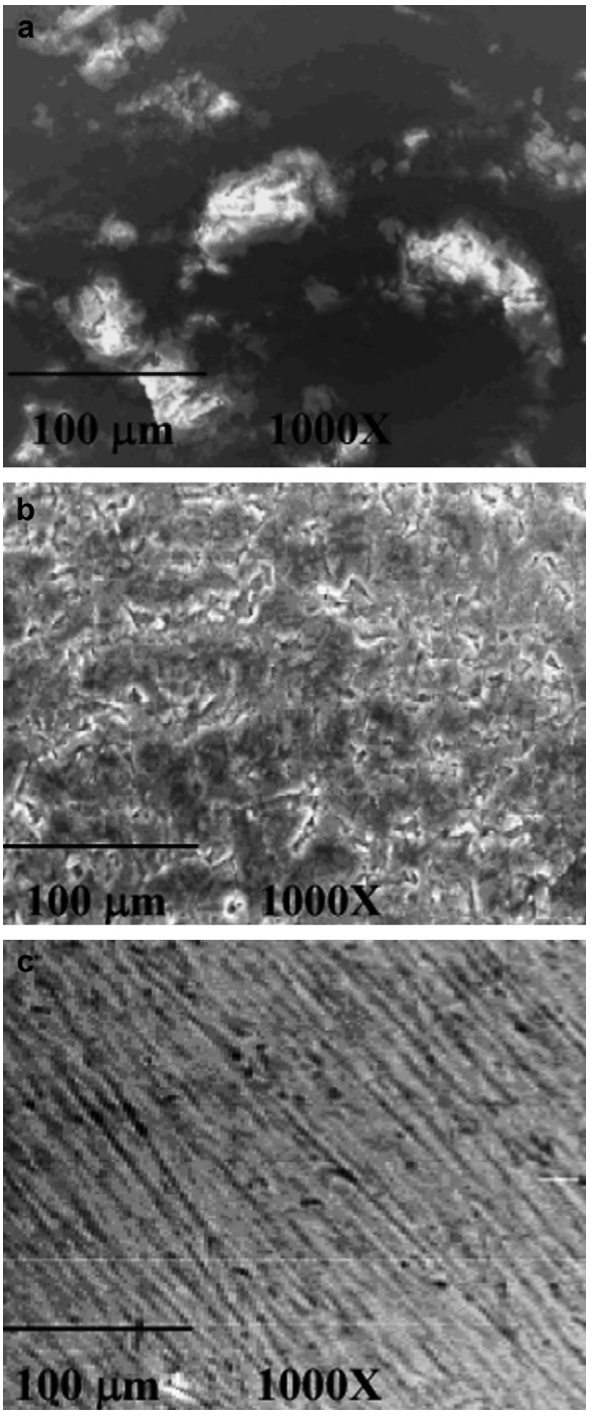

Fig. 14 – SEM micrographs for steel alloy after 100 h of immersion in blank solution (a) without inhibitors (b) with 0.01 mM of compound II and (c) with 0.01 mM of compound I at 1000X.

Also, both R_T and C_T^{-1} decrease with increasing temperature (Figs. 12 and 13), respectively which is in a good agreement with polarization data.

Generally, the results show that Compound I has lower corrosion rate than compound II than the blank. This was confirmed by Scanning electron microscope (SEM) images shown in Fig. 14a–c after 100 h of immersion in blank solution (a) without inhibitors (b) with 0.01 mM of inhibitor I and (c) with 0.01 mM of inhibitor II. It was shown that SEM image for the blank is corroded, then for compound I, there is a compact film formed on the surface. However, for compound II, the film formed on the surface is smoother than that for blank, but surface film formed for compound I is better than that formed for compound II.

4. Conclusions

The following main conclusions are drawn from the present study: Compound I has the lowest corrosion rate at 1.0 mM and compound II at 6.0 mM concentration, however, compound I always has lower corrosion rate than compound II. The order of inhibition is: I > II. According to the values of K_{ads}, strongest interaction between the double layer existing at the phase boundary, the adsorbed molecules gives the highest *IE*% for compound I. The two inhibitors show an adsorption on steel surface according to the Langmuir adsorption isotherm. The values of ΔG°_{ads} of the two compounds indicating that the two compounds adsorb on steel surface via a physisorption-based mechanism.

Acknowledgment

The authors are grateful to Chemistry Department, Cairo University, for supporting this work.

REFERENCES

[1] Valcarce MB, Vázquez M. Carbon steel passivity examined in alkaline solutions: the effect of chloride and nitrite ions. Electrochemica Acta 2008;53:5007.
[2] Ergun Ü, Yüzer D, Emregül KC. The inhibitory effect of bis-2,6-(3,5-dimethylpyrazolyl)pyridine on the corrosion behavior of mild steel in HCl solution. Materials Chemistry and Physics 2008;109:492.
[3] Fekry AM, Ameer MA. Corrosion inhibition of mild steel in acidic media using newly synthesized heterocyclic organic molecules. International Journal of Hydrogen Energy 2010;35:7641.
[4] Altaf F, Qureshi R, Ahmed S, Khan Y, Naseer A. Electrochemical adsorption studies of urea on copper surface in alkaline medium. Electroanalytical Chemistry 2010;642:98.
[5] Elsener B. Corrosion inhibitors for steel in concrete, state of the art report. EFC Publication 35, The Institute of Materials. London: Maney Publishing; 2001.
[6] Fekry AM, Abdel Hamid RM. Electrochemical impedance studies of modified Ni–P and Ni–P–Cu deposits in alkaline medium. Electrochimica Acta 2010;55:5922.
[7] Alonso C, Castellote M, Andrade C. Chloride threshold dependence of pitting potential of reinforcements. Electrochimica Acta 2002;47:3469.
[8] Abdel-Fattah A, Elneairy M, Gouda M, Attaby F. Synthesis, characterization, and reactions of pyridine-3-carbonitrile derivatives. Phosphorus, Sulfur, Silicon and Other Related Elements 2008;183:1592.

[9] Amin MA. Weight loss, polarization, electrochemical impedance spectroscopy, SEM and EDX studies of the corrosion inhibition of copper in aerated NaCl solutions. Journal of Applied Electrochemistry 2006;36:215.
[10] Yazici B, Tatli G, Galip H, Erbil M. Investigation of suitable cathodes for the production of hydrogen gas by electrolysis. International Journal of Hydrogen Energy 1995; 20:957.
[11] Obot IB, Obi-Egbedi NO, Umoren SA. The synergistic inhibitive effect and some quantum chemical parameters of 2,3-diaminonaphthalene and iodide ions on the hydrochloric acid corrosion of aluminium. Corrosion Science 2009;51:276.
[12] Saremi M, Mahallati E. A study on chloride-induced depassivation of mild steel in simulated concrete pore solution. Cement and Concrete Research 2002;32:1915.
[13] Saraby-Reintjes A. Theory of competitive adsorption and its application to the anodic dissolution of nickel and other iron-group metals—II. The steady state in the prepassive, passive and transpassive potential ranges. Electrochimica Acta 1985;30:403.
[14] Kim JD, Pyun SI. The effects of applied potential and chloride ion on the repassivation kinetics of pure iron. Corrosion Science 1996;38:1093.
[15] Fekry AM, Mohamed RR. Acetyl thiourea chitosan as an eco-friendly inhibitor for mild steel in sulphuric acid medium. Electrochimica Acta 2010;55:1933.
[16] Heakal FE, Fekry AM. Experimental and theoretical study of uracil and adenine inhibitors in Sn–Ag Alloy/nitric acid corroding system. Journal of Electrochemical Society 2008; 155:C534.
[17] Patrito E, Macagno V. Influence of the forming electrolyte on the electrical properties of anodic zirconium oxide films: part II. Ac impedance investigation. Journal of Electroanalytical Chemistry 1994;375:203.
[18] Fekry AM, Gasser AA, Ameer MA. Corrosion protection of mild steel by polyvinylsilsesquioxanes coatings in 3% NaCl solution. Journal of Applied Electrochemistry 2010;40:739.
[19] Davenport A, Oblonsky L, Ryan M. The structure of the passive film that forms on iron in aqueous environments. Journal of Electrochemical Society 2000;147:2162.
[20] Fekry AM. The influence of chloride and sulphate ions on the corrosion behavior of Ti and Ti-6Al-4V alloy in oxalic acid. Electrochimica Acta 2009;54:3480.
[21] Lunarska E, Chernyayeva O. Effect of corrosion inhibitors on hydrogen uptake by Al from NaOH solution. International Journal of Hydrogen Energy 2006;31:285.
[22] El-Meligi AA, Ismail N. Hydrogen evolution reaction of low carbon steel electrode in hydrochloric acid as a source for hydrogen production. International Journal of Hydrogen Energy 2009;34:91.
[23] Azizi O, Jafarian M, Gobal F, Heli H, Mahjani MG. The investigation of the kinetics and mechanism of hydrogen evolution reaction on tin. International Journal of Hydrogen Energy 2007;32:1755.
[24] Bhardwaj M, Balasubramaniam R. Uncoupled non-linear equations method for determining kinetic parameters in case of hydrogen evolution reaction following Volmer–Heyrovsky–Tafel mechanism and Volmer–Heyrovsky mechanism. International Journal of Hydrogen Energy 2008;33:2178.
[25] Proud WG, Muller C. The electrodeposition of nickel on vitreous carbon: impedance studies. Electrochimica Acta 1993;38:405.
[26] Beccaria A, Chiaruttini L. The inhibitive action of metacryloxypropylmethoxysilane (MAOS) on aluminium corrosion in NaCl solutions. Corrosion Science 1999;41:885.
[27] Migahed MA, Mohamed HM, Al-Sabagh AM. Corrosion inhibition of H-11 type carbon steel in 1 M hydrochloric acid solution by N-propyl amino lauryl amide and its ethoxylated derivatives. Materials Chemistry and Physics 2003;29:169.
[28] Chun JH, Jeon SK, Ra KH, Chun JY. The phase-shift method for determining Langmuir adsorption isotherms of over-potentially deposited hydrogen for the cathodic H_2 evolution reaction at poly-Re/aqueous electrolyte interfaces. International Journal of Hydrogen Energy 2005;30:485.